Technical University of Denmark

The Cobweb Effect in Balancing Markets with Demand Response

Larsen, Emil Mahler; Pinson, Pierre; Wang, Jianhui; Ding, Yi

Published in:
Proceedings of European Electricity Market Conference 2015

Publication date:
2015

The Cobweb Effect in Balancing Markets with Demand Response

Emil M. Larsen, Pierre Pinson, Jianhui Wang, Yi Ding, Jacob Østergaard

***Abstract*—Integration of renewable energy sources (RES) like wind into the power system is a high priority in many countries, but it becomes increasingly difficult as renewables reach a significant share of generation. Demand response (DR) can potentially mitigate some of these difficulties, but the best way to control and integrate DR into the power system remains an open question. Integration into existing electricity markets is one option, but dynamic pricing with DR has been observed to be unstable, resulting in oscillations in supply and demand. This so-called Cobweb effect is presented here using the market structure and measurements from the EcoGrid EU demonstration, where five minute electricity pricing is sent to 1900 houses. A new tool for quantifying volatility is presented, and the causes for volatility are investigated. A key outcome of this study shows that increases in social welfare due to DR appear to be limited by the cost of volatility in existing market structures.**

***Index Terms*—Demand response (DR), demand forecasting, real-time pricing, volatility, smart grid.**

NOMENCLATURE

$t \in T$	Index for time
$g \in G$	Index for conventional generation
$n \in N$	Index for demand model parameters
$s \in S$	Index for scenario
$q_{t,s}$	Scenario probability
$c_{t,s}$	Real-time demand
θ_n	Demand model parameters
θ_λ	Price-elasticity parameters
c_t^{D}	Day-ahead demand forecast
$c_{t,s}^{\lambda}$	Demand response
$c_{t,s}^{\mathrm{shed}}$	Load shedding
λ_t^{D}	Day-ahead price for demand
λ_t^{R}	Real-time price for demand
λ^{shed}	Price for load shedding
λ^{spill}	Price for wind spillage
$B_{t,s}$	System imbalance
$p_{g,t}^{\mathrm{D}}$	Conventional generation scheduled day-ahead
w_t^{D}	Wind power day-ahead forecast
$w_{t,s}^{\mathrm{spill}}$	Wind power spillage
$\lambda_{g,t}^{\uparrow}, \lambda_{g,t}^{\downarrow}$	Price for up/down regulation
$p_{g,t,s}^{\uparrow}, p_{g,t,s}^{\downarrow}$	Up/down regulation delivered
$P_{g,t}^{\uparrow}, P_{g,t}^{\downarrow}$	Up/down regulation bid into market
$n_{g,t,s}, m_{g,t,s}$	Up/down regulation on/off
$r_{g,t}$	Generator ramp rate

Manuscript submitted 11/05/2015. This work was partly supportly by the European Commission through the project EcoGrid EU (grant ENER/FP7/268199) and by Mogens Balslev's Foundation.

E. M. Larsen, P. Pinson and J. Østergaard are with the Centre for Electric Power and Energy, Technical University of Denmark, Kgs. Lyngby, Denmark (email: {emlar,ppin,joe}@elektro.dtu.dk). J. Wang is at Argonne National Laboratory, USA (email: {jianhui.wang@anl.gov}). Y. Ding is at Zhejiang University, China (email: {yiding@zju.edu.cn}.

I. INTRODUCTION

DEMAND response (DR) is being strongly pursued because it increases the value of renewable energy sources (RES) when they are available, provides some additional capacity when renewables are not available, and balances the system when renewables do not behave as predicted [1]. In Denmark, the shift to RES meant that wind power met 39% of national electricity consumption in 2014, and is well on its way to hitting goals of 50% electricity consumption from wind power in 2020, and 100% of all energy consumption from renewable energy in 2050 [2].

There are many dynamic and static electricity price tariffs that can be used to activate DR, but two methods in particular have gained traction in recent years due to their fast activation characteristics that compliment the uncertainty in RES generation. These are direct control, where utilities turn devices on and off remotely, and indirect control, where an incentive signal, e.g. an electricity price, is used to influence the load to change its consumption. Direct control is typically targeted at medium and large commercial and industrial loads and has the challenges of requiring reliable communication equipment, while indirect control is aimed at a large number of small-scale loads and has challenges of predictability [3], [4]. Key benefits of indirect control include lower equipment costs and, when a price-based mechanism is used, there can be a clear value attributed to the resource. When used in conjunction with a market, indirect control has the additional benefit of improving liquidity and lowering the cost of supply, since it reduces the market power of price-maker generators. However, true market-based pricing sent to supply and demand has long been associated with unstable behavior, as first identified in [5], where it was named the Cobweb effect due to the spider web-like back-and-forth oscillations that occur when a stable market equilibrium cannot be achieved.

The Cobweb effect has traditionally been studied in markets where demand for a commodity, for example apples, was higher or lower than supply had expected. The following season, apple growers then change their production level, but the market becomes over- or under-supplied and an overshoot causes demand to behave in a seemingly opposite fashion to what had been experienced the previous season. If every market participant has a perfect forecast of supply and demand, then the Cobweb effect should not happen, but uncertainty is usually present in markets. This is true in a modern power system and especially true for DR [6]. Electricity market clearing algorithms must also make assumptions about demand, including linearising non-linear behavior, in order to find a feasible and timely solution in an optimization framework. This can result in power and prices being more volatile than is optimal, as seen in Fig. 1. Here, an imbalance that exists only at the first time step where supply and demand intersect, oscillates outwards as the initial decision leads to a greater imbalance (feedback) in subsequent steps.

In this paper, we investigate the Cobweb effect using the market structure and data collected from the EcoGrid EU project, which is an indirect control demonstration on the Danish island of Bornholm. The EcoGrid EU demonstration has 1900 residential households with a peak load of 5MW. Houses are equipped with smart meters and a range of distributed energy resources (DERs) with automated controllers that receive a new electricity price every five minutes and optimize consumption levels accordingly. DR from these customers is scheduled optimally with manual reserves from conventional generation in a market structure to meet the imbalance caused by wind power. A mathematical introduction to the EcoGrid EU market can be found in [7].

The contribution of this work lies in identifying the different causes of volatility, identifying volatility in realistic real-time market that respects Scandinavian generation constraints and was developed in conjunction with the Danish Transmission System Operator (TSO), Energinet.dk, and developing an intuitive method for measuring volatility. We also investigate the impact the Cobweb effect has on social welfare, and the influence market re-commitment frequency has on volatility and social welfare. We believe the latter to be important as system operators move to shorter settlement periods, like the five minute period in the novel EcoGrid EU market.

The paper is structured with section II presenting existing knowledge of the Cobweb effect. Section III describes the simulation components, which include a model of the demand based on EcoGrid EU measurements, the market structure,

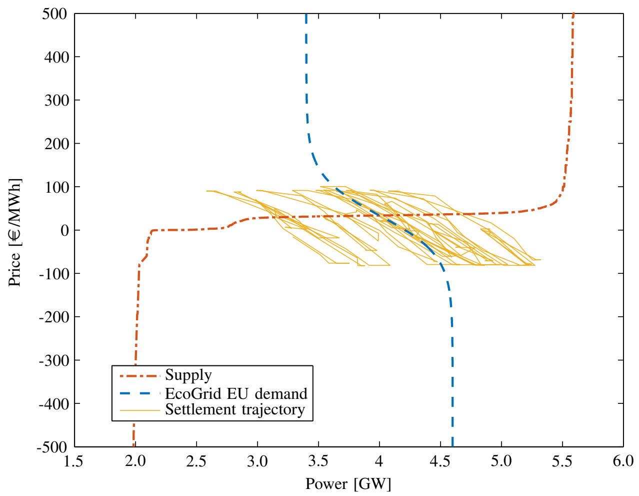

Fig. 1. The Cobweb effect in the EcoGrid EU market, where the settlement trajectory starts at the intersection of the initial supply (Nord Pool bid data) and demand (EcoGrid EU demand model) curves shown.

and a tool for measuring volatility. Section IV presents results for social welfare and volatility from simulations and the real experiment. The final section concludes.

II. The Cobweb effect

Since initially investigated in 1938, the Cobweb effect was expanded to markets with non-linear supply and demand curves in [8], where it was also shown that the Cobweb effect happens with monotonic demand and supply curves, as is the case in electricity markets. In [9], the impact of demand expectation using auto-regressive methods on the Cobweb effect was identified. Traditional economics literature has been more focused on identifying the problem and improving the expectation of demand, including considering larger forecast horizons, leading to more stable market outcomes [10]. Solutions other than a better demand forecast have not been explored. Recent economics research on the Cobweb effect has moved to analyzing games between different players, the result of which is an equilibrium with the lowest forecast error on both the supply and demand side [11].

In the field of power system research, market-based volatility due to real-time pricing was first identified in [12], where it was noted that there is an upper limit on the market clearing time and the delay of the price signal beyond which the system becomes unstable. Here it was shown that delaying communication of the price sent to customers increased system stability greatly, while increasing the gate-closure time led to fragile system behavior. Cobweb-like volatility has been particularly problematic when using models from the New York ISO power system [13], however, the authors there used a mirror image of supply to represent demand in the absence of reliable information about its actual shape. In addition, authors there also assumed demand would only be non-linear with respect to time, but not conditional on past and future prices.

Recently, [14] identified the boundaries for volatility when closed-loop real-time pricing structures are used without an appropriate feedback law. No remedy was offered for the closed-loop instabilities simulated in this research, but it was noted that price volatility increases as the price-elasticity of consumers increases with respect to the price-elasticity of suppliers, indicating that volatility will vary from power system to power system. Real data was not used in [14], highlighted by a demand profile with eight peaks per day, rather than the archetypal one or two daily peaks. Consequently, there remains a lack of evidence about how much volatility will truly be observed in a power system with DR and real-time pricing, hence our curiosity as to whether the Cobweb effect is observable or significant in a realistic market setup.

III. Methodology

In this section, a model of demand based upon the data collected in the EcoGrid EU demonstration is described. The market structure is presented and measures for volatility are defined. The demand model is used with the market to simulate several weeks of operation assuming that indirect control was rolled-out nationwide in Denmark.

A. Model of the Demand

Demand is broken down into non-interacting parts comprised of autoregressive components that are a function of recent demand, a component that is dependent on the price, and a component that is only dependent on external variables using the notation from [15], [16]. An initial abstract split of the price and non-price responsive parts is considered,

$$c_t = f\left(\tilde{c}_{t-1}, \tilde{z}_t\right) + g\left(\tilde{\lambda}_t, \tilde{z}_t\right) \tag{1}$$

with

$$\begin{aligned}\tilde{c}_{t-1} &= \left[c_{t-1}, \dots, c_{t-n_c}\right]^\top \\ \tilde{\lambda}_t &= \left[\lambda_{t+u_\lambda}, \dots, \lambda_{t-n_\lambda}\right]^\top \\ \tilde{z}_t &= \left[z_{t+u_z}, \dots, z_{t-n_z}\right]^\top\end{aligned}$$

where n_c, n_λ and n_z are a finite number of lagged values of demand, c, price, λ, and external variables, z respectively. For the price and external variables there are u_λ and u_z forecast values, which capture the scheduling dynamics of DERs. External variables, z, include weather data such as temperature, wind speed, and solar irradiance, as well as a base load term, y. The base load is a Fourier series that describes demand due to the time of day, day of the week, and day of the month [17], such that, for a given time t,

$$y_t = a_0 + \sum_{j=1}^{J} a_j \sin\left(\frac{2\pi kt}{j}\right) + b_j \cos\left(\frac{2\pi kt}{j}\right) \tag{2}$$

The cardinality of j must be suitably large to cover different seasonal variations (for example 288 when capturing trends of different hours of the day using five minute data) and k is increased until enough high-resolution detail is captured.

The full model for demand can be expressed in general linear model form, i.e.

$$c_t = \tilde{c}_{t-1}^\top \theta_c + \tilde{\lambda}_t^\top \theta_\lambda + \tilde{z}_t^\top \theta_z \epsilon_t = x_t^\top \boldsymbol{\theta} + \epsilon_t \tag{3}$$

where ϵ_t is Gaussian noise with zero mean and finite variance. Variables c, λ and z were populated with measurements from 2014 and the parameters $\boldsymbol{\theta}$ of the general linear model were found by minimizing the residual sum of squares while shrinking parameters using the Lasso penalisation [18], the objective of which is

$$\min \sum_{t=1}^{T} \left(c_t - \sum_{i=1}^{I} \theta_i x_{i,t}\right)^2 + \eta \sum_{i=1}^{N} |\theta_i| \tag{4}$$

where η is the tuning parameter and is found using a 10-fold cross-validation routine, minimising the error over all folds. Fig. 2 shows the main outcome of the price terms in the general linear model for the coldest six months of the year. DR peaks 20 minutes after the price change, and the main response lasts for 90 minutes before a rebound effect is observed. Smart controllers prepare in the hour preceding price change by scheduling an opposing response, causing load to shift.

The relationship between price and demand has previously been observed to be non-linear [15], and we model this by

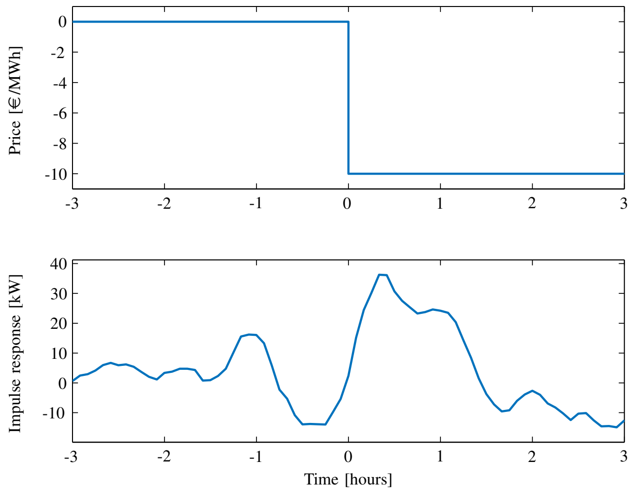

Fig. 2. Finite impulse response (FIR) of the EcoGrid EU demand in 2014, corresponding to the parameters θ_λ peaking at 36kW when given a € 10 price decrease at t_0.

redefining the price terms in a generalised logistic function that is centred around zero, i.e.

$$c_t^\lambda = \sum_{t=1}^{n_\lambda} -\frac{A_t}{2} + \frac{A_t}{1 + e^{-\varepsilon_t \lambda_t}} \tag{5}$$

where c_t^λ contains only price information with other linear components removed. Parameters in this model are found by minimising the sum of square errors using the Levenberg-Marquardt algorithm [19], with the linear parameters for price used as starting estimates for ε. The upper and lower bounds of the price response are the amplitude of the logistic function and are defined with respect to the instantaneous price only (at $t = 1$), so that

$$c_t^{\lambda,\max} = \frac{|A_1|}{2} \tag{6}$$

$$c_t^{\lambda,\min} = -\frac{|A_1|}{2} \tag{7}$$

The final demand model exhibits a non-linear response to price and behaves dynamically according to future and past prices. The model has been used to forecast demand in real-time in the EcoGrid EU demonstration, with a five-minute ahead mean absolute percentage error (MAPE) of under 2% for 1900 houses.

B. Market Structure

The EcoGrid EU demonstration has two hardware in-the-loop market steps, as shown in Fig. 3, which were used to generate five minute electricity pricing for 1900 houses in 2014 and 2015. Generator bids are based on historical Nord Pool bid data, as shown in Fig. 1, while inflexible demand and wind power injection comes from commercial real-time forecasts. The imbalance signal is derived from the day-ahead wind power forecast error, scaled by the Danish nominal capacity, which is around 5%.

The first step is a day-ahead market that minimizes the cost of conventional generation, considering the day-ahead wind power production forecast, the known Nord Pool spot price, and the demand forecast including price-response to spot prices. It is not the main area of focus, because it does not generate the day-ahead price and demand is a fixed input. This step is only needed to find reasonable and feasible starting points for generators participating in the real-time market. The overall problem reads

$$\min \sum_{g,t} \lambda_{g,t} p^{\mathrm{D}}_{g,t} + \sum_{t} \lambda^{\mathrm{shed}} c^{\mathrm{shed}}_{t} - \sum_{t} \lambda^{\mathrm{spill}} w^{\mathrm{spill}}_{t} \tag{8a}$$

subject to

$$\sum_{g} p^{\mathrm{D}}_{g,t} + w^{\mathrm{D}}_{t} - w^{\mathrm{spill}}_{t} = c^{\mathrm{D}}_{t} - c^{\mathrm{shed}}_{t} \qquad \forall t \tag{8b}$$

$$p^{\mathrm{D}}_{g,t} \geq P^{\min}_{g} \qquad \forall g,t \tag{8c}$$

$$p^{\mathrm{D}}_{g,t} \leq P^{\max}_{g} \qquad \forall g,t \tag{8d}$$

$$p^{\mathrm{D}}_{g,t} - p^{\mathrm{D}}_{g,t-1} \leq r_{g,t} \qquad \forall g,t \tag{8e}$$

$$p^{\mathrm{D}}_{g,t-1} - p^{\mathrm{D}}_{g,t} \leq r_{g,t} \qquad \forall g,t \tag{8f}$$

Scheduled generation, day-ahead wind power forecasts, wind spillage, load shedding and day-ahead load forecasts are balanced in (8b). Wind power injection is a parameter that is treated as a negative load. Minimum and maximum generation is constrained in (8c) and (8d), while up and down ramp rates are bound by $r_{g,t}$ in (8e) and (8f).

The second market step is the novel EcoGrid EU market, where social welfare is maximized with respect to the day-ahead market outcome. The market schedules an optimal amount of manual reserves and flexible demand, and is formulated as a stochastic optimization problem that commits bids for conventional generation and creates real-time prices (RTP) for demand until the market is cleared again. Unscheduled and scheduled generation from the first market step is used as the up and down regulation bids respectively in the real-time market, i.e. $p^{\uparrow}_{g,t,s} = P^{\max}_{g} - p^{\mathrm{D}}_{g,t}$ and $p^{\downarrow}_{g,t,s} = p^{\mathrm{D}}_{g,t} - P^{\min}_{g}$. This yields

$$\max \sum_{t} \sum_{s} q_{t,s} \Bigg\{ \left(\lambda^{\mathrm{D}}_{t} c^{\lambda}_{t,s} + \mathrm{diag}\left(\theta_{t,t',s}\right) 0.5 {c^{\lambda}_{t,s}}^{2} \right) - \sum_{g} \beta_{g,t,s} - \lambda^{\mathrm{spill}} w^{\mathrm{spill}}_{t,s} - \lambda^{\mathrm{shed}} c^{\mathrm{shed}}_{t,s} \Bigg\} \tag{9a}$$

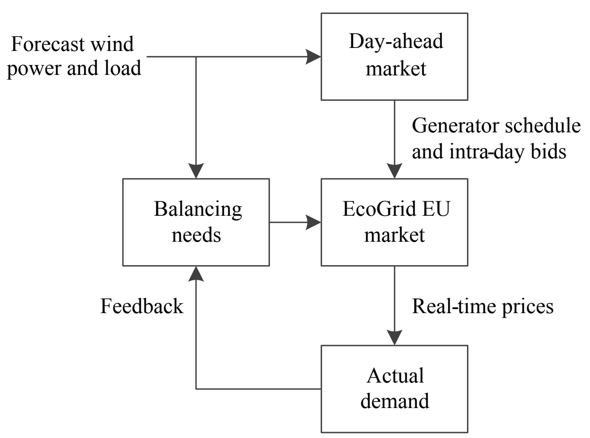

Fig. 3. Hardware-in-the-loop market structure of the EcoGrid EU demonstration.

subject to

$$c^{\lambda}_{t,s} = \sum_{t'} \left(\theta_{t,t',s} \left(\lambda^{\mathrm{R}}_{t} - \lambda^{\mathrm{D}}_{t} \right) \right) \qquad \forall t,s \tag{9b}$$

$$c^{\lambda}_{t,s} \leq c^{\lambda,\max}_{t} \qquad \forall t,s \tag{9c}$$

$$c^{\lambda}_{t,s} \geq c^{\lambda,\min}_{t} \qquad \forall t,s \tag{9d}$$

$$c^{\lambda}_{t,s} = 0 \qquad \forall s, t > h \tag{9e}$$

$$c_{t,s} = c^{\mathrm{D}}_{t} - c^{\mathrm{shed}}_{t,s} + c^{\lambda}_{t,s} \qquad \forall t,s \tag{9f}$$

$$w_{t} = w^{\mathrm{D}}_{t} - w^{\mathrm{spill}}_{t,s} \qquad \forall t,s \tag{9g}$$

$$\beta_{g,t,s} = \lambda^{\uparrow}_{g,t} p^{\uparrow}_{g,t,s} - \lambda^{\downarrow}_{g,t} p^{\downarrow}_{g,t,s} \qquad \forall g,t,s \tag{9h}$$

$$p_{g,t,s} = \sum_{g} p^{\mathrm{D}}_{g,t,s} + p^{\uparrow}_{g,t,s} - p^{\downarrow}_{g,t,s} \qquad \forall g,t,s \tag{9i}$$

$$c_{t,s} = p_{g,t,s} + w_{t,s} - B_{t,s} - e_{t} \qquad \forall t,s \tag{9j}$$

$$\Delta p^{\uparrow}_{g,t,s} = p^{\uparrow}_{g,t,s} - p^{\uparrow}_{g,t-1,s} \qquad \forall g,t,s \tag{9k}$$

$$\Delta p^{\downarrow}_{g,t,s} = p^{\downarrow}_{g,t,s} - p^{\downarrow}_{g,t-1,s} \qquad \forall g,t,s \tag{9l}$$

$$\Delta p^{\uparrow}_{g,t,s} = \Delta p^{\uparrow}_{g,t-1,s} \qquad \forall g,t,s,\gamma_{t} = 0 \tag{9m}$$

$$\Delta p^{\downarrow}_{g,t,s} = \Delta p^{\downarrow}_{g,t-1,s} \qquad \forall g,t,s,\gamma_{t} = 0 \tag{9n}$$

$$\Delta p^{\uparrow}_{g,t,s} = 0 \qquad \forall g,t,s,\gamma_{t} = 2 \tag{9o}$$

$$\Delta p^{\downarrow}_{g,t,s} = 0 \qquad \forall g,t,s,\gamma_{t} = 2 \tag{9p}$$

$$p^{\uparrow}_{g,t,s} \leq n_{g,t,s} p^{\uparrow}_{g,t,s} \qquad \forall g,t,s \tag{9q}$$

$$p^{\downarrow}_{g,t,s} \leq m_{g,t,s} p^{\downarrow}_{g,t,s} \qquad \forall g,t,s \tag{9r}$$

$$p^{\uparrow}_{g,t,s} \geq n_{g,t,s} \chi_{g} p^{\uparrow}_{g,t,s} \qquad \forall g,t,s,\gamma_{t} = 2 \tag{9s}$$

$$p^{\downarrow}_{g,t,s} \geq m_{g,t,s} \chi_{g} p^{\downarrow}_{g,t,s} \qquad \forall g,t,s,\gamma_{t} = 2 \tag{9t}$$

$$n_{g,t,s} = 0 \qquad \forall t,s,P^{\uparrow}_{g,t} = 0 \tag{9u}$$

$$m_{g,t,s} = 0 \qquad \forall t,s,P^{\downarrow}_{g,t} = 0 \tag{9v}$$

$$p^{\uparrow}_{g,t,s} \leq d_{t,s} p^{\uparrow}_{g,t,s} \qquad \forall g,t,s \tag{9w}$$

$$p^{\downarrow}_{g,t,s} \leq l_{t,s} p^{\downarrow}_{g,t,s} \qquad \forall g,t,s \tag{9x}$$

$$d_{t,s} + l_{t,s} \leq 1 \qquad \forall g,t,s,\gamma_{t} = 2 \tag{9y}$$

The objective function (9a) maximises social welfare, where the first term is customer utility and the last terms are cost of generation and slack variables. Customer utility includes the instantaneous price-elasticity, $\mathrm{diag}\left(\theta_{t,t'}\right)$, and the change in consumption due to all past and future prices, c^{λ}_{t}. The full finite impulse response (FIR) for price, θ_{λ}, which comes from the demand model, is contained t' times in the square matrix $\left(\theta_{t,t'}\right)$, where the diagonal term represents t = 1 of the FIR. Each price contribution to the load is summed for all cross-elasticities in constraint (9b), giving the total DR and the real-time price for demand, λ^{R}_{t}. The EcoGrid EU market produces separate prices for supply and demand when supply and demand constraints are reached (e.g. generator ramping), but identical ones when such constraints are not binding. Actors that caused the imbalance receive the average price for balancing power from supply and demand.

When cross-elasticity is ignored, as in Scandinavia today and in the original EcoGrid EU design, then only the diagonal term in $\theta_{t,t'}$ is non-zero, and is fixed to the average FIR from the general linear model parameters (3) until the market is cleared again, i.e. if the market is run hourly, then the first 12 values of the FIR after a price change are used to determine price elasticity, e.g.

$$\theta_\lambda = \frac{1}{12}\sum_{n=1}^{12}\frac{1}{\theta_{\lambda_n}} \tag{10}$$

Clearing an electricity market considering cross-elasticity is not needed in today's deregulated power systems because the loads that participate in existing DR schemes have a cross-elastic time constant that is longer than the re-commitment time of the system they participate in. For example, a factory that reduces its consumption for an hour to meet the terms of a DR contract will not compensate for this reduction in the following hour, since it will cause an imbalance and be penalised as a result. Instead, its cross-elastic time constant depends on long term planning ranging from days to years, far slower than day-ahead and real-time markets recommit bids today. Small-scale DR, which indirect control leans towards, can have a time-constant of just a few minutes, as seen in the EcoGrid EU demand model. This time-constant is a similar order of magnitude to the re-commitment frequency in real-time markets today, which suggests that cross-elastic effects must be fully incorporated into the market to obtain an economically efficient and controllable outcome.

A method for clearing a market considering the cross-elastic nature of the load was previously proposed in [20]. However, the algorithm used does not converge on a solution if the demand's self-elasticity is smaller than its cross-elasticity. This solution may work well in an hourly market, where the demand characteristics are likely to lead to a solution, but in a five minute market like EcoGrid EU, the cross-elastic terms are larger than the self-elastic terms, hence our proposed modified market structure.

Constraints (9c) and (9d) determine the flexible demand limits. Constraint (9e) sets DR to zero for twice the FIR length, $h = 2(u_\lambda + n_\lambda)$, so that market outcomes do not create infeasible starting points for subsequent re-commitments.

The total demand and production from wind are defined in (9f) and (9g). The regulating cost from conventional generation is defined in (9h). The total power produced by conventional generation is stated in (9i). Constraint (9j) is the balance constraint, also considering the imbalance from wind and inflexible demand, B_t, and feedback from the load, e_t. Constraints (9k) - (9y) dictate generator behavior like minimum on-times and ramping characteristics that are in-line with the Scandinavian regulating market today. Constraints (9k) and (9l) define generator ramp rates. Constraints (9m) and (9n) keep ramping constant for 15 minutes. Constraints (9o) and (9p) ensure that a generator is at a fixed setpoint for at least 15 minutes. When used with the generator behavior of $\gamma_t = \{1, 0, 0, 2, 0, 0, 1, 0, 0, 2, 0...\}$, (9k)-(9p) result in a minimum on-time of 45 minutes. Constraints (9q) and (9r) are maximum regulation constraints. Constraints (9s) and (9t) are minimum generation constraints. In the Scandinavian regulating market, bids under 10MW must be activated in full, while bids above 10MW can be activated in part; the proportion of each bid to be activated is described by the parameter χ_g. Constraints (9u) and (9v) ensure that a generator is off when it bids zero into the market. Constraints (9w) and (9x) determine whether any up or down generation is active, according to binary variables $d_{t,s}$ and $l_{t,s}$ respectively, and (9y) prevents simultaneous up and down regulation.

For each scenario-based decision variable there exists a non-anticipativity constraint that ensures its outcome is identical across all scenarios in the first few time periods for which prices are fixed, for example $t = 1 \dots 6$ if the market is cleared every half hour. Scenarios for imbalance, B, are generated using a non-parametric method. Bootstrapping is employed, where historical outcomes are sampled with replacement. Scenarios for price-elasticity are normally distributed and scenario reduction is done using the Fast Forward method [21].

Any imbalance after the market cleared is penalised by a primary frequency reserve (PFR) energy cost, which is set to the highest and lowest marginal cost for energy in each time period.

EcoGrid EU market clearing code in the GAMS language and without proprietary datasets is available in [22]. The main EcoGrid EU market is a mixed integer quadratically constrained program (MIQCP) solved using the CPLEX solver.

C. Quantifying Volatility

We propose quantifying volatility using a rainflow counting algorithm [23], which is traditionally used in material fatigue and battery ageing analysis. The rainflow counting algorithm is a simple but powerful tool and the result is intuitive; Whenever there is a change of sign in the signal of interest, a turning point is defined. The distance between turning points is measured and binned for similar distances to give the number of oscillations observed per day. The algorithm can be described as

1) Reduce the time-series to sequential peaks and troughs.
2) Conceptually rotate the time-series 90°, so that the time-series starts at the top and ends at the bottom.
3) Represent each peak and trough as the source of water that drips down the time-series.
4) Count the number of half-cycles by looking at where the drops of water end, which is when either
    a) The drop reaches the end of the time-series;
    b) The the drop merges with the flow from an earlier drop; or
    c) An opposite peak or trough of greater magnitude occurs.
5) Determine the distance of each half-cycle between its start and end.
6) Pair up half-cycles of equal distance but opposite effect (falling off a peak or trough).

In Fig. 4, trough half cycles are counted and the distance for each cycle is measured for a time-series of DR. The total number of full cycles (troughs plus peaks) in this example are 16, with an average amplitude of 80.6MW.

IV. Results

A. The cause of the Cobweb effect

The main cause for the Cobweb effect is uncertainty, but this can be further specified as structural uncertainty, that is

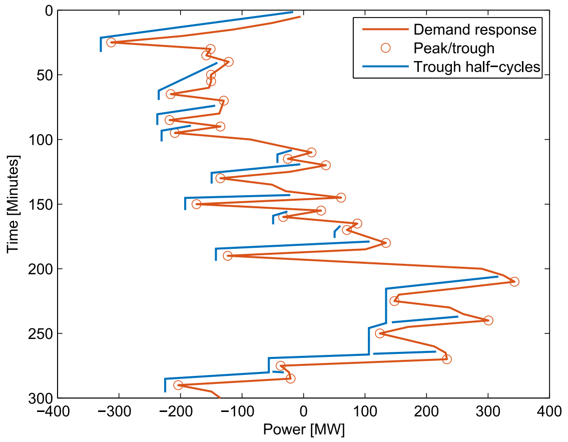

Fig. 4. Rainflow counter, where the black lines are half-cycles used count the number and amplitude of oscillations.

the linearisation of demand characteristics to fit into a market structure, and aleatoric uncertainty, which is the intrinsic randomness in natural processes. Structural uncertainty in our system comes from the non-linear demand curve, assumed to be linear in the market, and ignoring cross-elastic effects in the market.

To understand which source of uncertainty causes the greatest volatility, we performed simulations for Denmark for one month for a range of different cases. The first case is one with no DR. The second case is an open loop system, where feedback is ignored by the market and left for faster moving reserves like PFR to remedy. An open loop is unrealistic, because it requires no uncertainty in the source of an imbalance, and undesirable, because it requires larger PFR capacity. The next case is a closed loop system, where the market is run as was originally designed, and feedback from an unexpected response creates a new imbalance in subsequent market recommitments. In the fourth and fifth cases (Closed NL and CE), feedback from non-linear and cross-elastic behaviour is remedied by the market, one at a time, while the other is left as an open loop imbalance. This allows us to identify which is the bigger cause of the Cobweb effect. The sixth case (Closed M) simulates a full closed loop but with a modified market, where the full cross-elastic effects are modelled in our novel market constraint (9b). Finally, demonstration results are included. The demonstration cannot be directly compared to simulated cases because it uses a local imbalance signal, is subject to additional price delays, and is a pseudo-closed loop where delayed meter data is used to update the demand forecast.

Fig. 5 shows a simulation day with outcomes demand price and consumption, regulating price for generation, and regulating power activated respectively. In a closed-loop system, oscillating behaviour is seen in both generation and load. In an open loop system, similar volatility as the closed loop system can be seen in the first few hours of demand price, but this does not translate to volatility on the generation side. Increased volatility is therefore not a problem in itself from a market perspective - DR increases volatility of the demand even when expectation of demand is perfect, and this is to be cherished if DR is to help balance volatile renewable energy production. However, increased activation of regulating power is a clear indicator of the Cobweb effect in action.

Table I summarises the number of cycles counted by the rainflow counting algorithm for different cases. There is an increase in demand cycles across all scenarios with DR, which occurs naturally as the demand becomes dynamic. There is a reduction in supply cycles for all DR cases, which should be interpreted as fewer regulating bids being committed, which in turn means that DR has achieved its goal of reducing reliance on conventional power generation. The closed loop experiences the most volatile pricing, as it has the most supply price cycles.

Table II shows the cycle amplitude summed per day. For supply and demand, this relates to the total amount of balancing power activated, and for prices, this represents the sum of

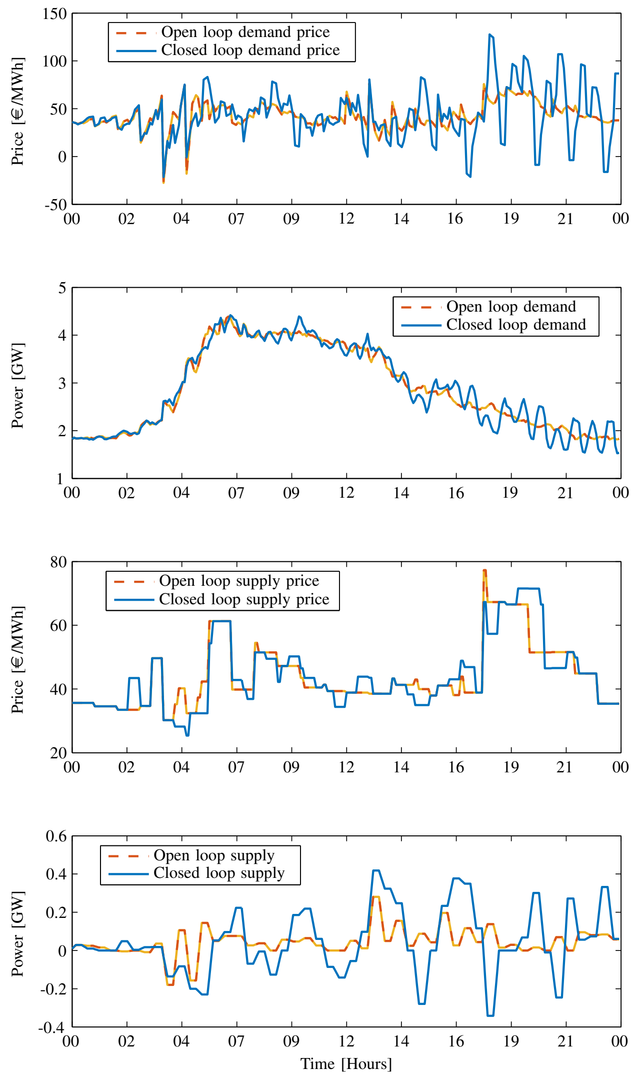

Fig. 5. Prices and power for supply and demand for an open- and closed-loop simulation day.

changes in activation price. Higher demand cycle amplitudes in all DR cases suggests load shifting is occurring. Real-time price amplitudes are lowest in the open loop and the Closed NL case, suggesting they behave in a similar manner and that feedback from a non-linear demand curve is less significant for volatility. In the original closed loop design and the Closed CE case, demand price amplitude is quadruple the open loop case. Daily supply and supply price amplitudes paint a similar picture, with the greatest volatility in the cases with feedback from cross-elasticity, and less volatility in the non-linear feedback case. The modified case should be directly compared to the closed loop case, where it exhibits half the supply volatility and a reduction of 46% in supply price. Despite this, it exhibits higher supply amplitudes (but at a lower price) than the zero-DR case, suggesting the Cobweb effect is still present here, but the market is able to exploit lower generation cost in spite of volatility.

B. Demand response penetration

To see if the Cobweb effect increases cost, cases were simulated for different levels of DR penetration. DR penetration was scaled from 0% to 100%, as shown in Fig. 6. The upper limit assumes that all of Denmark behaves like an EcoGrid EU load and represents a DR peak response about twice that of DR in the Nord Pool day-ahead market today, albeit with significantly more activations due to a lower price-elasticity characteristic (i.e. DR is cheaper to activate). DR penetration beyond 30% results in a reduction in social welfare in the closed-loop system, as the cost of volatility outweighs the benefit of DR. The case where feedback stems from cross-elastic effects (Closed CE) results in equally low social welfare, while the case where only non-linear effects are feedback has a very similar result to the open loop case. As with the rainflow counting results, this confirms that cross-elasticity is a bigger cause of the Cobweb effect than the non-linear demand curve. Finally, the modified market, which is a full closed loop, successfully increases social welfare for all levels of DR penetration. At low levels of DR penetration, social welfare gains are very small compared to the other cases because the modified market treats DR far more rigidly with fewer activations when it knows that a rebound will occur after 90 minutes. Lower DR activations means that costly conventional generator bids are activated instead, when leaving residual imbalances to faster moving reserves might have been more cost efficient.

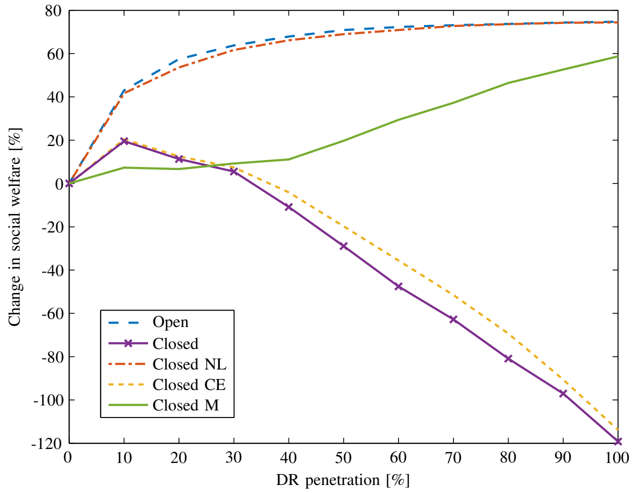

Fig. 6. Social welfare as a function of DR penetration. There is a reduction in social welfare as DR reaches significant proportions in closed-loop cases that do not account for a cross-elastic response.

Fig. 6 shows that DR has the potential to significantly increase social welfare in a real-time market, but only when cross-elasticity is explicitly optimized for in the market. However, this result should be moderated by the fact that revenue here is significantly smaller than in the day-ahead market, where DR volumes are less according to the EcoGrid EU demand model. In addition, this result is only applicable to the winter months when DR from heating in Denmark is expected to be active, so the year-round gain will be lower. The results are also highly dependent on assumptions about the supply curve; should DR become a significant reality, it's possible that bidding strategies would evolve.

C. Market re-commitment frequency

System dynamics change as system operators move to shorter settlement periods, like five minutes in the EcoGrid EU market, shorter gate-closure times, and more regular unit re-commitments to reduce the impact of RES uncertainty. We investigated re-commitment frequency by increasing how often the market was cleared from 15 minutes to 150 minutes in 15 minute intervals. The settlement period remains five minutes throughout (i.e. prices and set-points are valid for five minutes at a time), but new decisions are only taken every time the

TABLE I
AVERAGE CYCLES PER DAY

	Demand [Cycles]	Demand price [Cycles]	Supply [Cycles]	Supply price [Cycles]
No DR	62.9	0	20.4	13.1
Open	58.6	56.8	15.9	10.8
Closed	39.6	38.9	18.1	15.7
Closed NL	56.1	56.1	15.9	10.8
Closed CE	36.7	39.4	16.9	14.8
Closed M	75.0	88.6	17.1	13.9
Demo	65.9	73.3	24.5	15.0

TABLE II
AVERAGE SUM OF CYCLE AMPLITUDES PER DAY

	Demand [GWh]	Demand price [€/MWh]	Supply [GWh]	Supply price [€/MWh]
No DR	1.9	0	1.4	141.5
Open	4.3	482.8	1.1	91.5
Closed	16.1	2013.8	4.7	217.9
Closed NL	4.7	507.7	1.2	98.7
Closed CE	15.6	2122.0	4.2	224.9
Closed M	5.2	1690.3	2.3	133.1
Demo	3.8	125.2	3.6	72.9

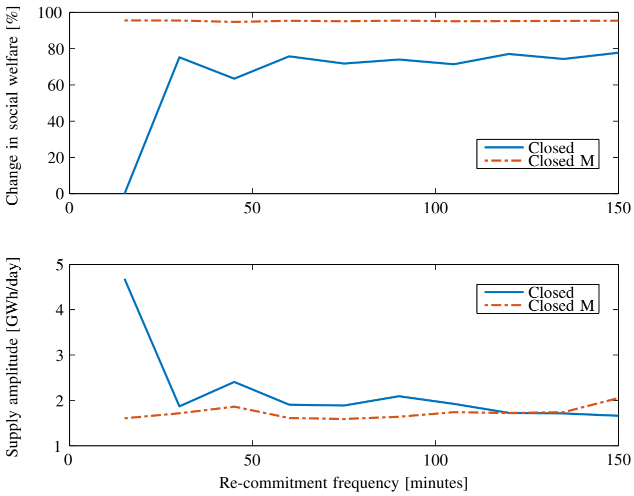

Fig. 7. Social welfare increases and volatility decreases as the re-commitment frequency is reduced in the standard closed-loop case.

market is cleared. The theoretical benefit of using a higher re-commitment frequency is that newer forecasts with less uncertainty can be used, leading to lower costs and therefore higher social welfare. Fig. 7 shows the outcome of changing unit commitment frequency on generation volatility and social welfare. The cross-elastic market exhibits similar behaviour for all timings, while the closed loop market actually exhibits lower volatility and higher social welfare for longer re-commitment intervals, which is the opposite to what would traditionally be expected. Volatility here translates to more generator bids being activated for more frequent re-commitments. The local peak in volatility at 45 minutes suggests also that the market clearing frequency is resonating with the minimum-on time for generation, and highlights additional market design challenges.

V. Conclusion

We have provided evidence that the Cobweb effect impacts the EcoGrid EU market, provoking costly oscillations on the supply side. In our case, the Cobweb effect causes three times more generator bids to be activated than in a market with no DR, leading to higher costs and lower social welfare. We observed that the non-linear demand curve does cause the Cobweb effect, but not enough to reduce social welfare. However, ignoring cross-elasticity in a market does lead to significant volatility and reduced social welfare. To mitigate this, we have directly incorporated cross-elasticity into the optimization problem. Such a solution may appear obvious, yet new, DR-focussed market designs that ignore cross-elasticity continue to appear in the literature [7], [24]. Reducing re-commitment frequency may be another option for reducing the Cobweb effect.

The question remains whether markets are the right tool to control fast-moving, non-linear DR. Our market and demand models are unlikely to capture all sources of volatility, and our measure for social welfare does not count all the costs that stem from it. Voltage and frequency instability could result from a seemingly small amount of volatility, and future research should determine how much volatility is acceptable.

Acknowledgment

The authors thank Henrik Bylling for scenario reduction advice. We thank DMI and ECMWF for weather forecasts, and Nord Pool and ENFOR for market data and power system forecasts respectively.

References

[1] Ea Energianalyse, "The future requirements for flexibility in the energy system," 2012.
[2] "Energistatistik 2011," Danish Energy Agency, Tech. Rep., 2011.
[3] K. Heussen, S. You, B. Biegel, L. H. Hansen, and K. B. Andersen, "Indirect control for demand side management - A conceptual introduction," *IEEE PES Innov. Smart Grid Technol. Conf. Eur.*, pp. 1–8, 2012.
[4] N. O'Connell, P. Pinson, H. Madsen, and M. O'Malley, "Benefits and challenges of electric demand response: A critical review," *Renew. Sustain. Energy Rev.*, vol. 39, pp. 686–699, 2014.
[5] M. Ezekiel, "The cobweb theorem," *Q. J. Econ.*, vol. 52, no. 2, pp. 255–280, 1938.
[6] J. L. Mathieu, D. S. Callaway, and S. Kiliccote, "Examining uncertainty in demand response baseline models and variability in automated responses to dynamic pricing," in *IEEE Conf. Decis. Control Eur. Control Conf.* IEEE, Dec. 2011, pp. 4332–4339.
[7] Y. Ding, S. Pineda, P. Nyeng, J. Ø stergaard, E. M. Larsen, and Q. Wu, "Real-time market concept architecture for EcoGrid EU - A prototype for European smart grids," *IEEE Trans. Smart Grid*, vol. 4, no. 4, pp. 2006–2016, 2013.
[8] C. H. Hommes, "Dynamics of the cobweb model with adaptive expectations and nonlinear supply and demand," *J. Econ. Behav. Organ.*, vol. 24, no. 3, pp. 315–335, 1994.
[9] C. H. Hommes, "On the consistency of backward-looking expectations: The case of the cobweb," *J. Econ. Behav. Organ.*, vol. 33, no. 3, pp. 333–362, 1998.
[10] D. Dufresne and F. Vázquez-Abad, "Cobweb theorems with production lags and price forecasting," *Econ. Discuss. Pap.*, no. 2012-17, 2012.
[11] J. Sonnemans, C. Hommes, J. Tuinstra, and H. Velden, "The instability of a heterogeneous cobweb economy: A strategy experiment on expectation formation," *J. Econ. Behav. Organ.*, vol. 54, no. 4, pp. 453–481, 2004.
[12] J. Nutaro and V. Protopopescu, "The impact of market clearing time and price signal delay on the stability of electric power markets," *IEEE Trans. Power Syst.*, vol. 24, no. 3, pp. 1337–1345, 2009.
[13] R. Masiello, J. Harrison, and R. Mukerji, "Market dynamics of integrating demand response into wholesale energy markets," *Electr. J.*, vol. 26, no. 6, pp. 8–19, 2013.
[14] M. Roozbehani, M. A. Dahleh, and S. K. Mitter, "Volatility of power grids under real-time pricing," *IEEE Trans. Power Syst.*, vol. 27, no. 4, pp. 1926–1940, 2012.
[15] O. Corradi, H. Ochsenfeld, H. Madsen, and P. Pinson, "Controlling electricity consumption by forecasting its response to varying prices," *IEEE Trans. Power Syst.*, vol. 28, no. 1, pp. 421–429, 2012.
[16] G. Dorini, P. Pinson, and H. Madsen, "Chance-constrained optimization of demand response to price signals," *IEEE Trans. Smart Grid*, vol. 4, no. 4, pp. 2072–2080, 2012.
[17] S. A.-h. Soliman and A. M. Al-Kandari, *Electrical load forecasting: Modeling and model construction*. Elsevier, 2010.
[18] G. James, D. Witten, T. Hastie, and R. Tibshirani, *An introduction to statistical learning*. Springer, 2006, vol. 102.
[19] J. Nocedal and S. J. Wright, *Numerical optimization*. Springer, 2006.
[20] C. D. Jonghe, B. F. Hobbs, and R. Belmans, "Optimal generation mix with short-term demand response and wind penetration," *IEEE Trans. Power Syst.*, vol. 27, no. 2, pp. 830–839, 2012.
[21] N. Growe-Kuska, H. Heitsch, and W. Romisch, "Scenario reduction and scenario tree construction for power management problems," *2003 IEEE Bol. Power Tech Conf. Proc.*, vol. 3, pp. 152–158, 2003.
[22] E. M. Larsen, "EcoGrid EU market clearing simulation code," 2014. [Online]. Available: https://github.com/emillarsen
[23] S. Downing and D. Socie, "Simple rainflow counting algorithms," *Int. J. Fatigue*, no. January, pp. 31–40, 1982.
[24] A. G. Vlachos and P. N. Biskas, "Demand response in a real-time balancing market clearing with pay-as-bid pricing," *IEEE Trans. Smart Grid*, vol. 4, no. 4, pp. 1966–1975, 2013.